

YANG–BAXTER EQUATIONS

Jacques H.H. Perk & Helen Au-Yang, Department of Physics, Oklahoma State University,
Stillwater, OK 74078-3072, USA

Introduction

The term Yang–Baxter Equations (YBE) has been coined by Faddeev in the late 1970s to denote a principle of integrability, i.e. exact solvability, in a wide variety of fields in physics and mathematics. Since then it has become a common name for several classes of local equivalence transformations in statistical mechanics, quantum field theory, differential equations, knot theory, quantum groups, and other disciplines. We shall cover the various versions and their relationships, paying attention also to the early historical development.

Electric networks

The first such transformation came up as early as 1899 when the Brooklyn engineer Kennelly published a short paper, entitled *the equivalence of triangles and three-pointed stars in conducting networks*. This work gave the

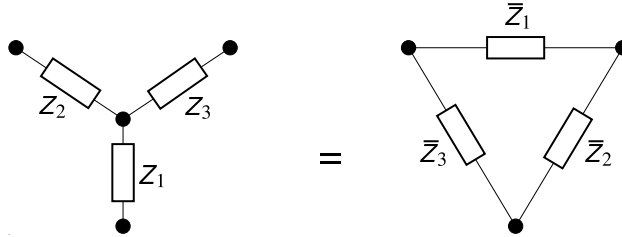


Figure 1: Star-triangle equation for impedances.

definite answer to such questions as whether it is better to have the three coils in a dynamo—or three resistors in a network—arranged as a star or as a triangle, see figure 1. Using Kirchhoff’s laws, the two situations in figure 1 can be shown to be equivalent provided

$$\begin{aligned} Z_1 \bar{Z}_1 &= Z_2 \bar{Z}_2 = Z_3 \bar{Z}_3 \\ &= Z_1 Z_2 + Z_2 Z_3 + Z_3 Z_1 & [1] \\ &= \bar{Z}_1 \bar{Z}_2 \bar{Z}_3 / (\bar{Z}_1 + \bar{Z}_2 + \bar{Z}_3) & [2] \end{aligned}$$

Here one has to take either [1] or [2] as second line of the equation, depending which direction the transformation is to go. The *star-triangle transformation* thus defined is also known under other names within the electric network theory literature as wye-delta ($Y - \Delta$), epsilon-delta ($\Upsilon - \Delta$), or tau-pi ($T - \Pi$) transformation.

Spin models

When Onsager wrote his monumental paper on the Ising model published in 1944, he made a brief remark on *an obvious star-triangle transformation* relating the model on the honeycomb lattice with the one on the triangular lattice. His details on this were first presented in Wannier's review article of 1945. However, the star-triangle transformation played a much more crucial role in Onsager's reasoning, as it is also intimately connected with his elliptic function uniformizing parametrization.

Furthermore, it implies the commutation of transfer matrices and spin-chain hamiltonians. Only in his Battelle lecture of 1970 did Onsager explain how he used this remarkable observation in his derivation of the formula for the spontaneous magnetization which he had announced as a conference remark in 1948 and of which the first complete derivation had been published by Yang in 1952 using a completely different method.

Many other applications and generalizations have since appeared. Most generally, we can consider a system whose state variables—also called spins—take values from some suitable discrete or continuous sets. The interactions between spins a and b are given in terms of weight factors W_{ab} and \overline{W}_{ab} , which are complex numbers in general, see figure 2. One quantity of special interest is the partition function—sum of the product of all weight factors over all allowed spin values. The integrability of the model is expressed by the existence of spectral variables—rapidities p, q, r, \dots —that live on oriented lines, two of which cross between a and b as indicated by the dotted lines in figure 2. Arrows from a to b are added to keep track of the ordering of a and b in case the weights are chiral (not symmetric).

In Onsager's special Ising model case the spins take values $a, b, c, \dots = \pm 1$ and the weight factors are the usual real positive Boltzmann weights depending on the product $ab = \pm 1$, uniformizing variable $p - q$ and elliptic modulus k . In the integrable chiral Potts model the weights depend on $a - b \bmod N$, with $a, b = 1, \dots, N$, whereas the rapidities p and q are living in general on a higher-genus curve.

When the weights are asymmetric in the spins, there are two sets of star-

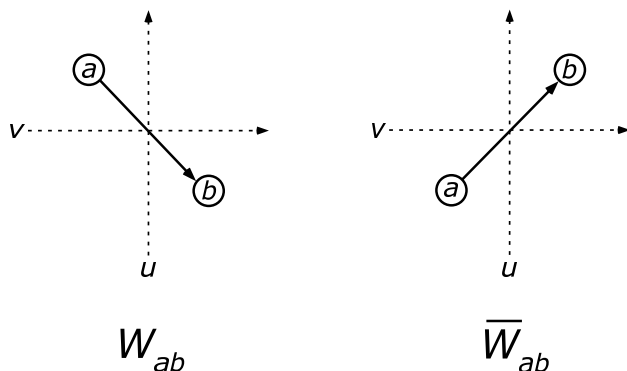


Figure 2: Spin model weights $W_{ab}(p, q)$ and $\overline{W}_{ab}(p, q)$.

triangle equations which can be expressed both pictorially—see figure 3—and algebraically:

$$\begin{aligned} \sum_d \overline{W}_{cd}(p, q) \overline{W}_{ab}(q, r) W_{da}(p, r) \\ = R(p, q, r) W_{ba}(p, q) W_{ca}(q, r) \overline{W}_{cb}(p, r) \end{aligned} \quad [3]$$

$$\begin{aligned} \overline{R}(p, q, r) W_{ab}(p, q) W_{ac}(q, r) \overline{W}_{bc}(p, r) \\ = \sum_d \overline{W}_{dc}(p, q) \overline{W}_{bd}(q, r) W_{ad}(p, r) \end{aligned} \quad [4]$$

Note that eqs. [3] and [4] differ from each other by the transposition of both spin variables in all six weight factors. In general there may also appear scalar factors $R(p, q, r)$ and $\overline{R}(p, q, r)$, which can often be eliminated by a suitable renormalization of the weights. If a , b , and c take values in the same set, we can sum over $a = b = c$ showing that $R = \overline{R}$ in that case.

The Kennelly star-triangle equation [1], [2] can be recovered as a special limit of a spin model where the states are continuous variables.

Knot theory and braid group

A seemingly totally different situation occurs in the theory of knots, links, tangles, and braids. In 1926 Reidemeister showed that only three types of moves suffice to show the equivalence between two different configurations, see figure 4. Moves of type I—removing simple loops—do not apply to braids.

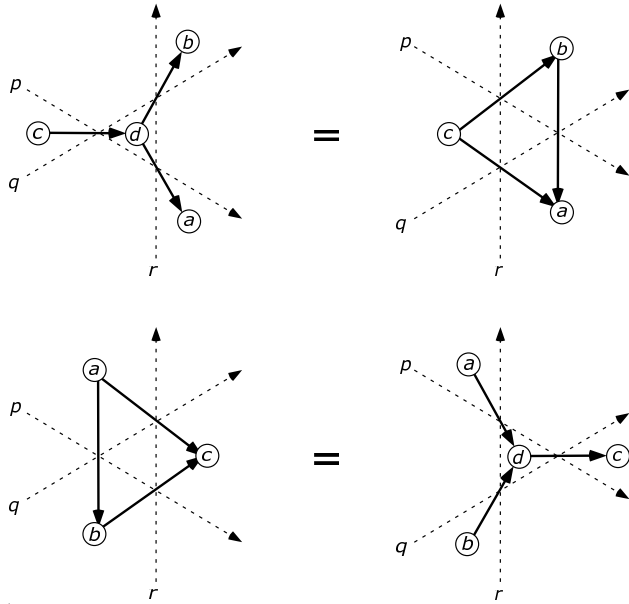


Figure 3: Star-triangle equation.

Moves of type II, for which one strand crosses twice over another strand, can be reformulated for braids, namely that an over-crossing is the inverse of an under-crossing. The Reidemeister move of type III is a precursor of the more general Yang–Baxter moves and can be represented also by the defining relations of Artin’s braid group. Let $R_{i,i+1}$ be the operator representing the situation in which the strand in position i crosses over the one in position $i + 1$. Then a braid can be represented by a product of $R_{j,j+1}$ ’s and their inverses, provided

$$R_{i,i+1}R_{i+1,i+2}R_{i,i+1} = R_{i+1,i+2}R_{i,i+1}R_{i+1,i+2} \quad [5]$$

and

$$[R_{i,i+1}, R_{j,j+1}] = 0, \quad \text{if } |i - j| \geq 2 \quad [6]$$

and similar relations in which $R_{i,i+1}$ and/or $R_{i+1,i+2}$ are replaced by their inverses.

Factorizable S-matrices and Bethe Ansatz

In the early 1960s Lieb and Liniger solved the one-dimensional Bose gas with delta-function interaction using the Bethe Ansatz. Yang and McGuire then

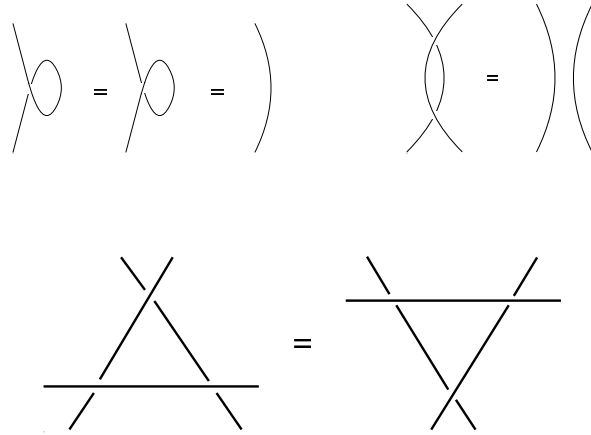


Figure 4: Reidemeister moves of type I, II, and III.

tried to generalize this result to systems with internal degrees of freedom and to fermions. This led to the discovery of the condition for factorizable S -matrices by McGuire in 1964, represented pictorially by figure 5. Here the worldlines of the particles are given. Upon collisions the particles can only

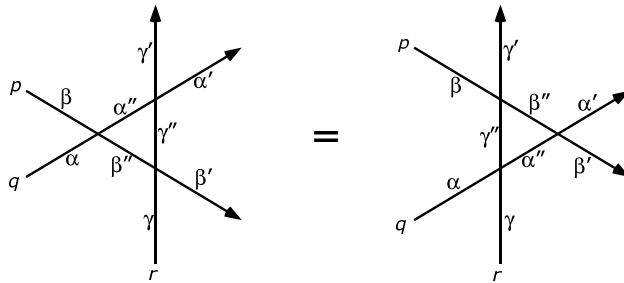


Figure 5: Vertex model Yang–Baxter equation.

exchange their rapidities p, q, r , so that there is no dispersion. Also indicated are the internal degrees of freedom in Greek letters. In other words, the three-body S -matrix can be factorized in terms of two-body contributions and the order of the collisions does not affect the final outcome. McGuire also realized that this condition is all you need for the consistency of factoring the n -body S -matrix in terms of two-body S matrices. The consistency condition is obviously related to the Reidemeister move of type III in figure 4.

Yang succeeded in solving the spin- $\frac{1}{2}$ fermionic model using a nested Bethe Ansatz, utilizing a generalization of Artin's braid relations [5] and [6],

$$\begin{aligned} & \check{R}_{i,i+1}(p-q)\check{R}_{i+1,i+2}(p-r)\check{R}_{i,i+1}(q-r) \\ &= \check{R}_{i+1,i+2}(q-r)\check{R}_{i,i+1}(p-r)\check{R}_{i+1,i+2}(p-q) \end{aligned} \quad [7]$$

He submitted his findings in two short papers in 1967. The \check{R} operators in eq. [7]—a notation introduced later by the Leningrad school—depend on differences of two momenta or two relativistic rapidities. Sutherland solved the general spin case using repeated nested Bethe Ansätze, while Lieb and Wu used Yang's work to solve the one-dimensional Hubbard model.

Vertex models

Since Lieb's solution of the ice model by a Bethe Ansatz there have been many developments on vertex models, in which the state variables live on line segments and a weight factors $\omega_{\alpha\mu}^{\lambda\beta}$ is assigned to a vertex where four line

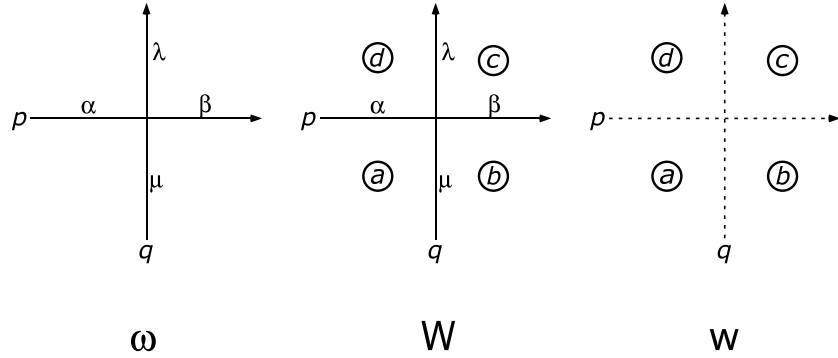


Figure 6: Vertex model weight $\omega_{\alpha\mu}^{\lambda\beta}(p, q)$, mixed model weight $W_{\alpha\mu|ab}^{\lambda\beta dc}(p, q)$ and IRF model weight $w_{ab}^{dc}(p, q)$.

segments with the four states $\alpha, \mu, \lambda, \beta$ on them meet, see figure 6.

Baxter solved the eight-vertex model in 1971, using a method based on commuting transfer matrices, starting from a solution of what he then called the generalized star-triangle equation, but what is now commonly called the Yang–Baxter equation (YBE):

$$\sum_{\alpha''} \sum_{\beta''} \sum_{\gamma''} \omega_{\beta\alpha}^{\alpha''\beta''}(p, q) \omega_{\alpha''\gamma''}^{\gamma'\alpha'}(q, r) \omega_{\beta''\gamma}^{\gamma''\beta'}(p, r)$$

$$= \sum_{\alpha''} \sum_{\beta''} \sum_{\gamma''} \omega_{\beta''\alpha''}^{\alpha'\beta'}(p, q) \omega_{\alpha''\gamma''}^{\gamma''\alpha''}(q, r) \omega_{\beta''\gamma''}^{\gamma'\beta''}(p, r) \quad [8]$$

This equation is represented graphically in figure 5. From it one can also derive a sufficient condition for the commutation of transfer matrices and spin-chain Hamiltonians, generalizing work of McCoy and Wu who had earlier initiated the search by showing that the general six-vertex model transfer matrix commutes with a Heisenberg spin-chain Hamiltonian. To be more precise, Baxter found that if $\omega_{\alpha\mu}^{\lambda\beta} = \delta_{\alpha}^{\lambda}\delta_{\mu}^{\beta}$ for some choice of p and q , some spin-chain Hamiltonians could be derived as logarithmic derivatives of the transfer matrix.

Interaction-Round-a-Face model

Baxter introduced another language, namely that of the “IRF-model” or “interaction-round-a-face” model, which he introduced in connection with his solution of the hard-hexagon model. This formulation is convenient when studying one-point functions using the corner-transfer-matrix method. Now

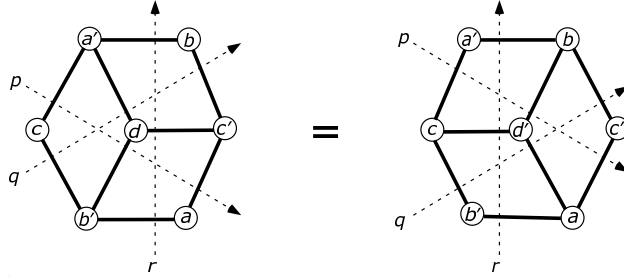


Figure 7: IRF model Yang–Baxter equation.

the integrability condition can be represented graphically as in figure 7 or algebraically as

$$\begin{aligned} & \sum_d w_{c'b'}^{a'd}(p, q) w_{d'c'}^{a'b}(q, r) w_{b'a}^{d'c'}(p, r) \\ &= \sum_{d'} w_{d'a}^{b'c'}(p, q) w_{b'a}^{c'd'}(q, r) w_c^{a'b}(p, r) \end{aligned} \quad [9]$$

The spins live on faces enclosed by rapidity lines and the weights $w_{ab}^{dc}(p, q)$ are assigned as in figure 6.

Baxter discovered a new principle based on eqs. 8 and 9, which he called Z -invariance as it expresses an invariance of the partition function Z under moves of rapidity lines. This also implies that typical one-point functions are independent of the values of the rapidities, while two-point functions can only depend on the values of the rapidities of rapidity lines crossing between the two spins considered. Many recent results on correlation functions in integrable models depend on this observation of Baxter.

IRF-vertex model

In figure 6, we have also defined mixed IRF-vertex model weights $W_{\alpha\mu}^{\lambda\beta|dc}(p, q)$. (We could put further state variables on the vertices, but then the natural thing to do is to introduce new effective weights summing over the states at each vertex.) With the choice made a more general Yang–Baxter equation

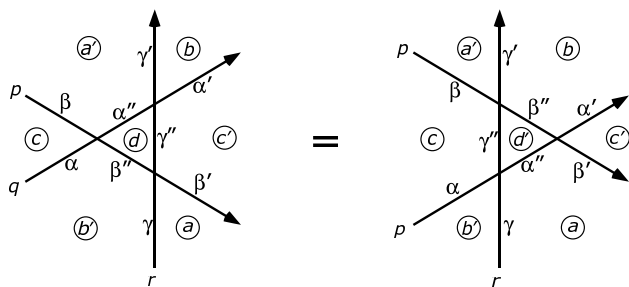


Figure 8: General Yang–Baxter equation.

can be represented as in figure 8, or by

$$\begin{aligned}
& \sum_{\alpha''} \sum_{\beta''} \sum_{\gamma''} \sum_d W_{\beta'' \alpha''}^{\alpha'' \beta'' | a' d} (p, q) \\
& \quad \times W_{\alpha'' \gamma''}^{\gamma'' \alpha'' | a' b} (q, r) W_{\beta'' \gamma''}^{\gamma'' \beta'' | d c'} (p, r) \\
& = \sum_{\alpha''} \sum_{\beta''} \sum_{\gamma''} \sum_{d'} W_{\beta'' \alpha''}^{\alpha'' \beta'' | b c'} (p, q) \\
& \quad \times W_{\alpha'' \gamma''}^{\gamma'' \alpha'' | c d'} (q, r) W_{\beta'' \gamma''}^{\gamma'' \beta'' | a' b} (p, r) \quad [10]
\end{aligned}$$

Quantum Inverse Scattering Method

The Leningrad school of Faddeev incorporated the methods of Baxter and Yang in their so-called *Quantum Inverse Scattering Method* (QISM), coining

the term *Quantum Yang–Baxter Equations* (QYBE) for the equations [8]. If special limiting values of p and q can be found, say as $\hbar \rightarrow 0$, such that $\omega_{\alpha\mu}^{\lambda\beta} = \delta_{\mu}^{\lambda}\delta_{\alpha}^{\beta} + O(\hbar)$, one can reduce [8] to the *Classical Yang–Baxter Equations* (CYBE) by expanding up to the first nontrivial order in expansion variable \hbar . These determine the integrability of certain models of classical mechanics by the inverse scattering method and the existence of Lax pairs.

Checkerboard generalizations

Star-triangle equations [3] and [4] imply that there are further generalizations of the Yang–Baxter equations, namely those for which the faces enclosed by the rapidity lines are alternately colored black and white in a checkerboard

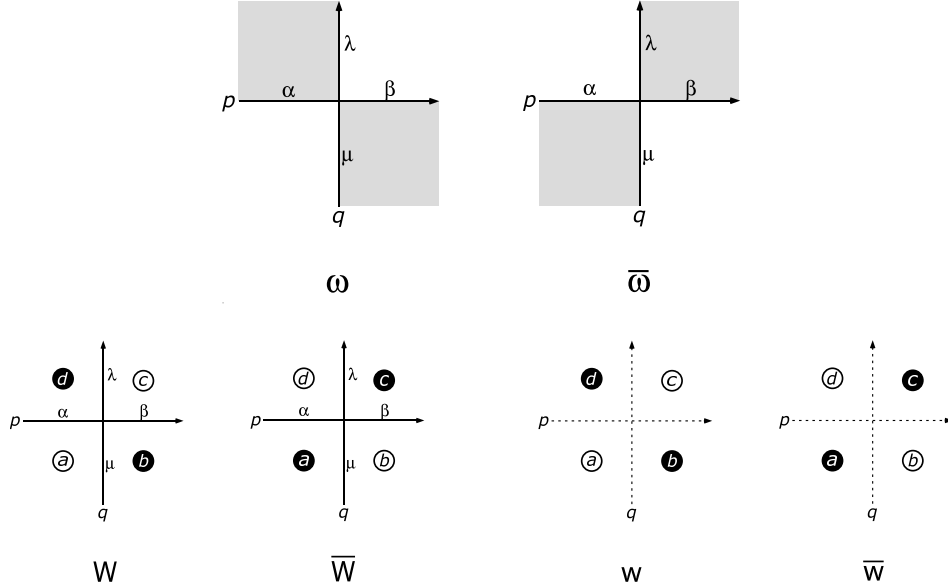


Figure 9: Checkerboard versions of the weights.

pattern. We can then introduce either vertex model weights $\omega_{\alpha\mu}^{\lambda\beta}(p, q)$ and $\bar{\omega}_{\alpha\mu}^{\lambda\beta}(p, q)$, or IRF-vertex model weights $W_{\alpha\mu}^{\lambda\beta|dc}(p, q)$ and $\bar{W}_{\alpha\mu}^{\lambda\beta|dc}(p, q)$, or IRF model weights $w_{ab}^{dc}(p, q)$ and $\bar{w}_{ab}^{dc}(p, q)$, see figure 9.

The black faces are those where the spins of the spin model with weights defined in figure 2 live; the white faces are to be considered empty in figures 2 and 3 (or, equivalently, they can be assumed to host trivial spins that take

on only a single value). Clearly, the IRF-vertex model description contains all the other versions.

Checkerboard vertex model

First we consider the checkerboard vertex model with weights $\omega_{\alpha\mu}^{\lambda\beta}(p, q)$ and $\bar{\omega}_{\alpha\mu}^{\lambda\beta}(p, q)$ as assigned in figure 9. The YBE [8] then generalizes to two sets of equations

$$\begin{aligned} & \sum_{\alpha''} \sum_{\beta''} \sum_{\gamma''} \omega_{\beta \alpha}^{\alpha'' \beta''}(p, q) \omega_{\alpha'' \gamma''}^{\gamma' \alpha'}(q, r) \bar{\omega}_{\beta'' \gamma''}^{\gamma'' \beta'}(p, r) \\ &= R(p, q, r) \sum_{\alpha''} \sum_{\beta''} \sum_{\gamma''} \bar{\omega}_{\beta'' \alpha''}^{\alpha' \beta'}(p, q) \\ & \quad \times \bar{\omega}_{\alpha \gamma}^{\gamma'' \alpha''}(q, r) \omega_{\beta \gamma''}^{\gamma' \beta''}(p, r) \end{aligned} \quad [11]$$

$$\begin{aligned} & \bar{R}(p, q, r) \sum_{\alpha''} \sum_{\beta''} \sum_{\gamma''} \bar{\omega}_{\beta \alpha}^{\alpha'' \beta''}(p, q) \\ & \quad \times \bar{\omega}_{\alpha'' \gamma''}^{\gamma' \alpha'}(q, r) \omega_{\beta'' \gamma''}^{\gamma'' \beta'}(p, r) \\ &= \sum_{\alpha''} \sum_{\beta''} \sum_{\gamma''} \omega_{\beta'' \alpha''}^{\alpha' \beta'}(p, q) \\ & \quad \times \omega_{\alpha \gamma}^{\gamma'' \alpha''}(q, r) \bar{\omega}_{\beta \gamma''}^{\gamma' \beta''}(p, r) \end{aligned} \quad [12]$$

where scalar factors R and \bar{R} have been added as in [3] and [4]. These equations are represented graphically by figure 10.

Checkerboard IRF model

The checkerboard IRF version of the YBE [8] becomes

$$\begin{aligned} & \sum_d w_c^{a'd}(p, q) w_d^{a'b}(q, r) \bar{w}_{b'a}^{d c'}(p, r) \\ &= R(p, q, r) \sum_{d'} \bar{w}_{d'a}^{b c'}(p, q) \bar{w}_{b'a}^{c d'}(q, r) w_c^{a'b}(p, r) \end{aligned} \quad [13]$$

$$\begin{aligned} & \bar{R}(p, q, r) \sum_d \bar{w}_c^{a'd}(p, q) \bar{w}_d^{a'b}(q, r) w_{b'a}^{d c'}(p, r) \\ &= \sum_{d'} w_{d'a}^{b c'}(p, q) w_{b'a}^{c d'}(q, r) \bar{w}_c^{a'b}(p, r) \end{aligned} \quad [14]$$

again with scalar factors R and \bar{R} added as in [3] and [4]. These equations can now be represented graphically as in figure 11. Note that these equations

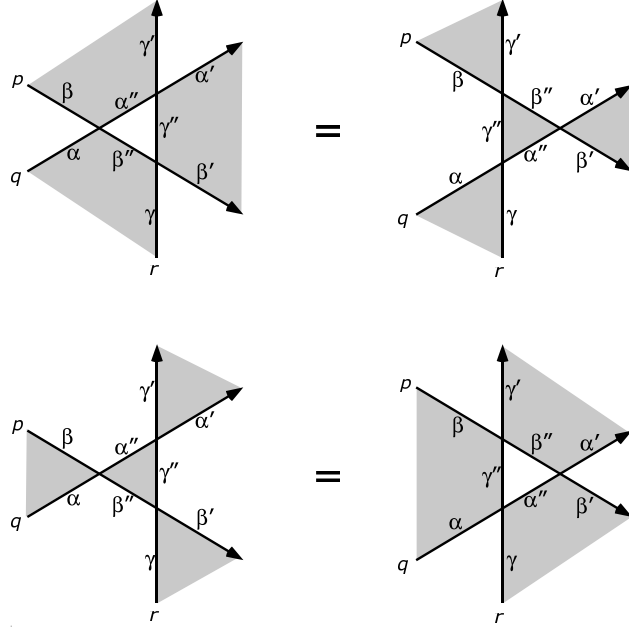


Figure 10: Checkerboard vertex model Yang–Baxter equation.

reduce to eqs. [3] and [4] if the spins on the white faces are allowed to take only one value, which means that they can be ignored.

Checkerboard IRF-vertex model

Finally, the most general case is represented by the checkerboard IRF-vertex model, with weights defined in figure 9. For this case the YBE are given by

$$\begin{aligned}
& \sum_{\alpha''} \sum_{\beta''} \sum_{\gamma''} \sum_d W_{\beta \alpha}^{\alpha'' \beta''} |_{c b'}^{a' d}(p, q) \\
& \quad \times W_{\alpha'' \gamma''}^{\gamma' \alpha'} |_{d c'}^{a' b}(q, r) \overline{W}_{\beta'' \gamma''}^{\gamma'' \beta'} |_{b' a}(p, r) \\
& = R(p, q, r) \sum_{\alpha''} \sum_{\beta''} \sum_{\gamma''} \sum_{d'} \overline{W}_{\beta'' \alpha''}^{\alpha' \beta'} |_{d' a}(p, q) \\
& \quad \times \overline{W}_{\alpha \gamma}^{\gamma'' \alpha''} |_{b' a}(q, r) W_{\beta \gamma''}^{\gamma' \beta''} |_{c d'}(p, r) \\
& \overline{R}(p, q, r) \sum_{\alpha''} \sum_{\beta''} \sum_{\gamma''} \sum_d \overline{W}_{\beta \alpha}^{\alpha'' \beta''} |_{c b'}(p, q) \\
& \quad \times \overline{W}_{\alpha'' \gamma''}^{\gamma' \alpha'} |_{d c'}(q, r) W_{\beta'' \gamma''}^{\gamma'' \beta'} |_{b' a}(p, r)
\end{aligned} \tag{15}$$

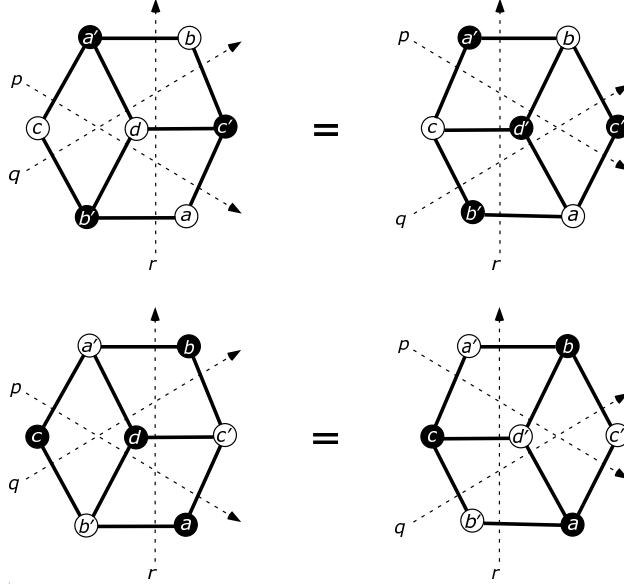


Figure 11: Checkerboard IRF model Yang–Baxter equation.

$$\begin{aligned}
&= \sum_{\alpha''} \sum_{\beta''} \sum_{\gamma''} \sum_{d'} W_{\beta''\alpha''|d'a}^{\alpha'\beta'}(p, q) \\
&\quad \times W_{\alpha\gamma|b'a}^{\gamma''\alpha''}(q, r) \overline{W}_{\beta\gamma''|c d'}^{\gamma'\beta''}(p, r)
\end{aligned} \tag{16}$$

with its graphical representation in figure 12.

Formal equivalence of languages

The square weight

Combining four weights of a checkerboard model in a square, as is done with four spin model weights in figure 13, we find a regular vertex model weight with rapidities that are now pairs of the original ones. In formula, this gives

$$\begin{aligned}
&W_{\alpha\mu}(p_1, q_1) \overline{W}_{\mu\beta}(p_1, q_2) \overline{W}_{\alpha\lambda}(p_2, q_1) W_{\lambda\beta}(p_2, q_2) \\
&= \omega_{\alpha\mu}^{\lambda\beta}(p_1, p_2; q_1, q_2)
\end{aligned} \tag{17}$$

From any solution of [3] and [4] we can construct a solution of YBE [8] this way. This has been used by Bazhanov and Stroganov to relate the integrable chiral Potts model with a cyclic representation of the six vertex model.

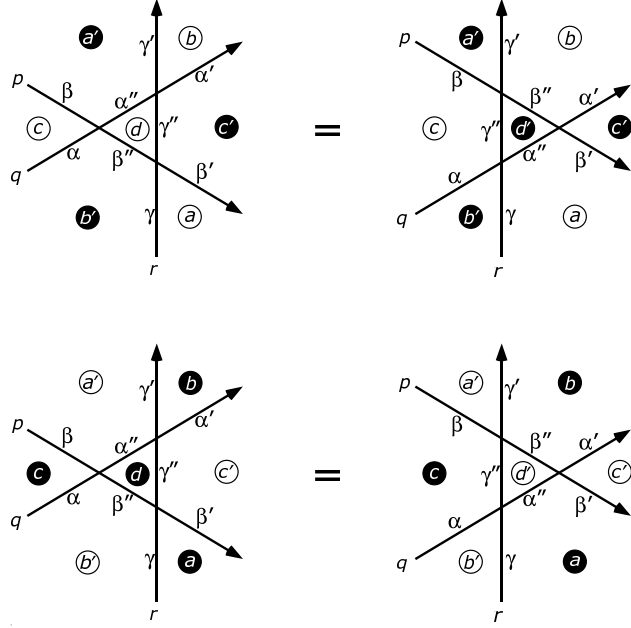


Figure 12: Checkerboard Yang–Baxter equation.

Map to checkerboard vertex model

The checkerboard IRF-vertex model formulation contains all other versions mentioned above as special cases. However, collecting the state variables in triples, we can immediately translate it to a vertex model version, writing

$$\omega_{\hat{\alpha}\hat{\mu}}^{\hat{\lambda}\hat{\beta}}(p, q) = W_{\alpha\mu}^{\lambda\beta|dc}(p, q), \quad \bar{\omega}_{\hat{\alpha}\hat{\mu}}^{\hat{\lambda}\hat{\beta}}(p, q) = \overline{W}_{\alpha\mu}^{\lambda\beta|dc}(p, q)$$

$$\text{if } \begin{cases} \hat{\lambda} = (d, \lambda, c), & \hat{\beta} = (b, \beta, c) \\ \hat{\alpha} = (a, \alpha, d), & \hat{\mu} = (a, \mu, b) \end{cases} \quad [18]$$

$$\omega_{\hat{\alpha}\hat{\mu}}^{\hat{\lambda}\hat{\beta}}(p, q) = \bar{\omega}_{\hat{\alpha}\hat{\mu}}^{\hat{\lambda}\hat{\beta}}(p, q) = 0 \quad \text{otherwise} \quad [19]$$

In eq. [19] we have set all vertex model weights zero that are inconsistent with IRF-vertex configurations. Clearly, the translation of IRF models and spin models to vertex models can be done similarly.

Map to spin model

We can furthermore translate each vertex model with weights assigned as in figures 6 or 9 into a spin model with weights as in figure 2 by defining

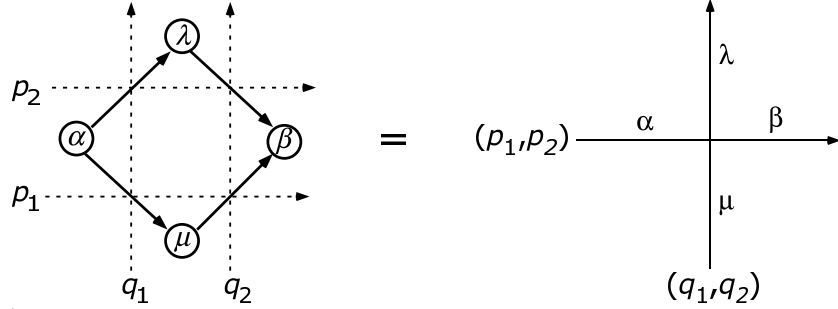


Figure 13: Square weight as vertex weight.

suitable spins in the black faces, after checkerboard coloring. Each spin is then defined to be the ordered set of states on the line segments of the vertex model, $\underline{a} = (\alpha_1, \alpha_2, \dots)$, ordering the line segments counterclockwise starting at, say, 12 o'clock. We can then identify $\omega_{\alpha\mu}^{\lambda\beta}(p, q) = W_{\underline{a}, \underline{b}}(p, q)$, $\bar{\omega}_{\alpha\mu}^{\lambda\beta}(p, q) = \bar{W}_{\underline{a}, \underline{b}}(p, q)$. This is surely not very economical, as many of the weights will be equal, but it helps show that all different versions of the checkerboard YBE are formally equivalent.

Hence, we shall only use the vertex-model language in the following. It is fairly straightforward to convert to the other formulations.

An $\mathfrak{sl}(m|\mathfrak{n})$ example

One fundamental example is a Q -state model for which the rapidities have $2Q+1$ components, $\vec{p} = (p_{-Q}, \dots, p_Q)$, $\vec{q} = (q_{-Q}, \dots, q_Q)$, etc., and the states on the line segments are arranged in strings of continuing conserved color. The vertex weights, for $\alpha, \beta, \lambda, \mu = 1, \dots, Q$, are given by

$$\omega_{\alpha\mu}^{\lambda\beta}(\vec{p}, \vec{q}) = \omega_{0\alpha\mu}^{\lambda\beta}(p_0, q_0) \frac{p_{+\lambda} q_{-\beta}}{q_{+\alpha} p_{-\mu}} \quad [20]$$

with

$$\begin{cases} \omega_0^{\rho\rho}(p_0, q_0) = \mathcal{N} \sinh[\eta + \varepsilon_\rho(p_0 - q_0)] \\ \omega_0^{\rho\sigma}(p_0, q_0) = \mathcal{N} G_{\rho\sigma} \sinh(p_0 - q_0), \quad \rho \neq \sigma \\ \omega_0^{\sigma\rho}(p_0, q_0) = \mathcal{N} e^{(p_0 - q_0)\text{sign}(\rho - \sigma)} \sinh \eta, \quad \rho \neq \sigma \\ \omega_0^{\lambda\beta}(p_0, q_0) = 0, \quad \text{otherwise} \end{cases} \quad [21]$$

where \mathcal{N} is an arbitrary overall normalization factor and η is a constant. Furthermore, $\varepsilon_\rho = \pm 1$ for $\rho = 1, \dots, Q$, with m of them equal $+1$ and n of them equal -1 . The $G_{\rho\sigma}$'s are constants satisfying $G_{\rho\sigma} = 1/G_{\sigma\rho}$, which freedom is allowed because the number of ρ - σ crossings minus the number of σ - ρ crossings is fixed by the states on the boundary only, i.e. the choice of $\alpha, \alpha', \beta, \beta', \gamma, \gamma'$ in YBE [8] and figure 5.

The solution [20], [21] has many applications. The case $m = 0, n = 2$ leads to the general six-vertex model; the $m = 0, n = n$ case produces the fundamental intertwiner of affine quantum group $U_q \widehat{\mathfrak{sl}}(n)$, whereas the case $m = 2, n = 1$ corresponds to the supersymmetric one-dimensional t - J model.

Operator formulations

The R -matrix

For a problem with N rapidity lines, carrying rapidities p_1, \dots, p_N , we can introduce a set of matrices $R_{ij}(p_i, p_j)$, for $1 \leq i < j \leq N$, with elements

$$R_{ij}(p_i, p_j)_{\alpha_1 \dots \alpha_N}^{\beta_1 \dots \beta_N} = \omega_{\alpha_i \alpha_j}^{\beta_i \beta_j}(p_i, p_j) \prod_{k \neq i, j} \delta_{\alpha_k}^{\beta_k} \quad [22]$$

In terms of these, the YBE [8] can be rewritten in matrix form as

$$\begin{aligned} R_{jk}(p_j, p_k) R_{ik}(p_i, p_k) R_{ij}(p_i, p_j) \\ = R_{ij}(p_i, p_j) R_{ik}(p_i, p_k) R_{jk}(p_j, p_k) \end{aligned} \quad [23]$$

where $1 \leq i < j < k \leq N$.

The \check{R} -matrix

If we transpose the β indices β_i and β_j in eq. [22], we can define a set of matrices $\check{R}_{i,i+1}(p, q)$ with elements

$$\check{R}_{i,i+1}(p, q)_{\alpha_1 \dots \alpha_N}^{\beta_1 \dots \beta_N} = \omega_{\alpha_i, \alpha_{i+1}}^{\beta_i, \beta_{i+1}}(p, q) \prod_{k \neq i, i+1} \delta_{\alpha_k}^{\beta_k} \quad [24]$$

Using these, the YBE [8] can be rewritten in matrix form as

$$\begin{aligned} \check{R}_{i,i+1}(q, r) \check{R}_{i+1, i+2}(p, r) \check{R}_{i, i+1}(p, q) \\ = \check{R}_{i+1, i+2}(p, q) \check{R}_{i, i+1}(p, r) \check{R}_{i+1, i+2}(q, r) \end{aligned} \quad [25]$$

and

$$[\check{R}_{i, i+1}(p, q), \check{R}_{j, j+1}(r, s)] = 0, \quad \text{if } |i - j| \geq 2 \quad [26]$$

In this formulation it is clear that many solutions can be found “Baxterizing” Temperley–Lieb and Iwahori–Hecke algebras.

Classical Yang–Baxter Equations

If we expand

$$\mathbf{R}_{ij}(p_i, p_j) = 1 + \hbar \mathbf{X}_{ij}(p_i, p_j) + O(\hbar^2) \quad [27]$$

in [23] we get in second order in \hbar the Classical Yang–Baxter Equation (CYBE) as the vanishing of a sum of three commutators, i.e.

$$\begin{aligned} & [\mathbf{X}_{ij}(p_i, p_j), \mathbf{X}_{ik}(p_i, p_k)] + [\mathbf{X}_{ij}(p_i, p_j), \mathbf{X}_{jk}(p_j, p_k)] \\ & + [\mathbf{X}_{ik}(p_i, p_k), \mathbf{X}_{jk}(p_j, p_k)] = 0 \end{aligned} \quad [28]$$

introduced by Belavin and Drinfel'd, where \mathbf{X}_{ij} is called the classical r -matrix.

Reflection Yang–Baxter Equations

Cherednik and Sklyanin found a condition determining the solvability of systems with boundaries, the Reflection Yang–Baxter Equations (RYBE), see figure 14. Upon collisions with a left or right wall the rapidity variable

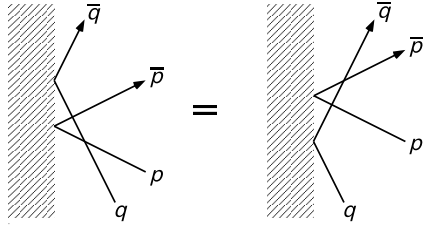


Figure 14: Reflection Yang–Baxter Equation.

changes from p to \bar{p} and back. In most examples, in which the rapidities are difference variables such that $\mathbf{R}(p, q) = \mathbf{R}(p - q)$, one also has $\bar{p} = \mu - p$, with μ some constant. The corresponding left boundary weights are $K_\alpha^\beta(p, \bar{p})$ satisfying

$$\begin{aligned} & \check{K}_1(q, \bar{q}) \check{R}_{12}(\bar{p}, q) \check{K}_1(p, \bar{p}) \check{R}_{12}(q, p) \\ & = \check{R}_{12}(\bar{p}, \bar{q}) \check{K}_1(p, \bar{p}) \check{R}_{12}(\bar{q}, p) \check{K}_1(q, \bar{q}) \end{aligned} \quad [29]$$

with $\check{K}_1(p, \bar{p})$ defined by a direct product as in [24] appending unit matrices for positions $i \geq 2$, and a similar equation must hold for the right boundary. Most work has been done for vertex models, while Pearce and coworkers wrote several papers on the IRF-model version.

Higher dimensional generalizations

In 1980 Zamolodchikov introduced a three-dimensional generalization of the YBE, the so-called Tetrahedron Equations (TE), and he found a special solution. Baxter then succeeded in proving that this solution satisfies all Tetrahedron Equations. Baxter and Bazhanov showed in 1992 that this solution can be seen as a special case of the $\mathfrak{sl}(\infty)$ chiral Potts model. Several authors found further generalizations more recently.

Inversion relations

When $\omega_{\alpha\mu}^{\lambda\beta}(p, p) \propto \delta_{\alpha}^{\lambda}\delta_{\mu}^{\beta}$, i.e. the weight decouples when the two rapidities are equal, one can derive the local inverse relation depicted in figure 15, which is

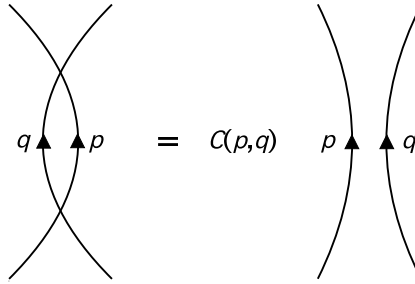


Figure 15: Local inversion relation.

a generalization of the Reidemeister move of type II in figure 4. It is easily shown that $C(q, p) = C(p, q)$.

This local relation implies also a global inversion relation which can be found in many ways. The following heuristic way is the easiest: Consider the situation in figure 16, with N closed p -rapidity lines and M closed q -rapidity lines. For M and N large, we may expect the partition function of figure 16 to factor asymptotically in top- and bottom-half contributions. If each line segment carries a state variable that can assume Q values, then the total partition function factors by repeated application of the relation in figure 15 into the contribution of $M + N$ circles. Therefore,

$$Z = Q^{M+N} C(p, q)^{MN} \approx Z_{M,N}(p, q) Z_{N,M}(q, p) \quad [30]$$

Taking the thermodynamic limit,

$$z(p, q) \equiv \lim_{M, N \rightarrow \infty} Z_{M,N}(p, q)^{1/MN} \quad [31]$$

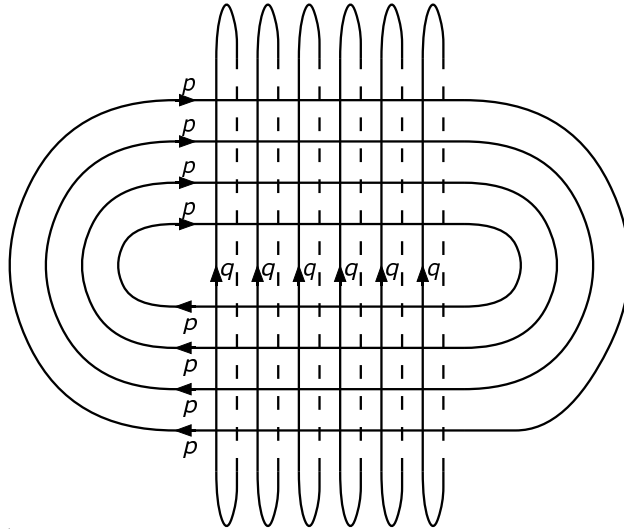


Figure 16: Heuristic derivation of inversion relation.

one finds

$$z(p, q)z(q, p) = C(q, p) \quad [32]$$

In many models eq. [32], supplemented with some suitable symmetry and analyticity conditions, can be used to calculate the free energy per site.

See also

Bethe Ansatz, Quantum groups, Ising model, Potts model, Vertex model, IRF model, Quantum inverse scattering method, Lax pair, Knot theory, Temperley–Lieb algebra, Factorisable S-matrix

Further Reading

Au-Yang H and Perk JHH (1989) Onsager’s star-triangle equation: Master key to integrability. *Advanced Studies in Pure Mathematics* 19: 57–94.

Baxter RJ (1982) *Exactly Solved Models in Statistical Mechanics*. Academic Press, London.

Behrend RE, Pearce PA, O’Brien DL (1996) Interaction-Round-a-Face Models with Fixed Boundary Conditions: The ABF Fusion Hierarchy. *J. Stat. Phys.* 84: 1–48.

- Gaudin M (1983) *La Fonction d'Onde de Bethe*. Masson, Paris.
- Jimbo M (ed) (1987) *Yang–Baxter Equation in Integrable Systems*. World Scientific, Singapore.
- Kennelly AE (1899) The equivalence of triangles and three-pointed stars in conducting networks. *Electrical World and Engineer* 34: 413–414.
- Korepin VE, Bogoliubov NM, and Izergin AG (1993) *Quantum Inverse Scattering Method and Correlation Functions*. Cambridge Univ. Press.
- Kulish PP and Sklyanin EK (1981) Quantum spectral transform method. Recent developments. In: Hietarinta J and Montonen C (eds) *Integrable quantum field theories*, Lecture Notes in Physics, vol. 151, pp 61–119. Springer, Berlin.
- Lieb EH and Wu FY (1972) Two-Dimensional Ferroelectric Models. In: Domb C and Green MS (eds) *Phase Transitions and Critical Phenomena*, vol. 1, pp 331–490. Academic Press, London.
- Onsager L (1971) The Ising model in two dimensions. In: Mills RE, Ascher E and Jaffee RI (eds) *Critical phenomena in alloys, magnets and superconductors*, pp xix–xxiv, 3–12. McGraw-Hill, New York.
- Perk JHH (1989) Star-triangle equations, quantum Lax pairs, and higher genus curves. *Proc. Symposia in Pure Math.* 49(1): 341–354.
- Perk JHH and Schultz CL (1981) New families of commuting transfer matrices in q -state vertex models. *Phys. Lett.* A84: 407–410.
- Perk JHH and Wu FY (1986) Graphical approach to the nonintersecting string model: star-triangle equation, inversion relation, and exact solution. *Physica* A138: 100–124.
- Reidemeister K (1926) Knoten und Gruppen. *Abh. Math. Sem. Hamburg. Univ.* 5: 7–23. Elementare Begründung der Knotentheorie. *ibid.* 24–32.
- Yang CN (1967) Some exact results for the many-body problem in one dimension with repulsive delta-function interaction. *Phys. Rev. Lett.* 19: 1312–1314.

Yang CN (1968) *S* Matrix for the One-Dimensional N -Body Problem with Repulsive or Attractive δ -Function Interaction. *Phys. Rev.* 167: 1920–1923.

Remark: most older work can be found from Jimbo’s book above, while most more recent work can be found at www.arXiv.org.

Appendix: Relation of resistor networks with Gaussian model and Potts model

We make next a few remarks on the relationship of resistor networks with related Gaussian models and Potts models in certain limits.

We start with a graph G with vertices j and edges $\langle j, j' \rangle$. We associate with each vertex j an electric potential ϕ_j and with each edge $\langle j, j' \rangle$ a resistance $R_{j,j'}$. According to Ohm’s law the current from vertex j to a neighboring vertex j' (i.e. $j' \in \text{Nb}_j$) is given by

$$I_{j,j'} = \frac{\phi_j - \phi_{j'}}{R_{j,j'}}, \quad [33]$$

whereas the power dissipated in the resistors is

$$P = \sum_{\langle j,j' \rangle} \frac{(\phi_j - \phi_{j'})^2}{R_{j,j'}}, \quad [34]$$

with a sum over all edges. Kirchhoff’s second law is implicit in this formulation. However, minimizing P over the potential ϕ_j for all internal vertices j (i.e. $j \in \text{Int}_G$), we find

$$\frac{\partial P}{\partial \phi_j} = 0 \quad \Longrightarrow \quad \sum_{j' \in \text{Nb}_j} \frac{\phi_j - \phi_{j'}}{R_{j,j'}} = 0 \quad \Longrightarrow \quad \sum_{j' \in \text{Nb}_j} I_{j,j'} = 0 \quad [35]$$

and Kirchhoff’s first law emerges.

We can now define the associated Gaussian model on graph G , using P for the interaction energy. The partition function is

$$Z = \left(\prod_{j \in \text{Int}_G} \sqrt{\frac{\beta}{\pi}} \int_{-\infty}^{\infty} d\phi_j \right) \exp \left(-\beta \sum_{\langle j,j' \rangle} \frac{(\phi_j - \phi_{j'})^2}{R_{j,j'}} \right), \quad [36]$$

which depends on the “potentials” of the exterior vertices. In the zero-temperature limit $\beta \rightarrow \infty$ the free energy tends to $\min P$, defining the equilibrium state of the resistor network.

We can even go further and derive a star-triangle relation for the Gaussian model. Doing a single Gaussian integration over ϕ_0 at the internal point 0 of the star with vertices $j = 0, 1, 2, 3$, we find

$$\begin{aligned} & \sqrt{\frac{\beta}{\pi}} \int_{-\infty}^{\infty} d\phi_0 \exp\left(-\beta \sum_{j=1}^3 \frac{(\phi_j - \phi_0)^2}{R_{j,0}}\right) \\ &= \left(\prod_{j=1}^3 \frac{R_{j,0}^{1/3}}{R_{j,j+1}^{1/6}}\right) \exp\left(-\beta \sum_{j=1}^3 \frac{(\phi_j - \phi_{j+1})^2}{R_{j,j+1}}\right) \end{aligned} \quad [37]$$

with $j+1 \equiv 1$ for $j=3$ and $R_{j,j+1}$ defined by

$$\frac{R_{j,j+1}}{R_{j,0}R_{j+1,0}} = \sum_{k=1}^3 \frac{1}{R_{k,0}}, \quad \text{for } j = 1, 2, 3. \quad [38]$$

The front factor in the RHS of [37] has been factorized this way using the product of [38] over $j = 1, 2, 3$. It is related to the scalar factors $R(p, q, r)$ and $\bar{R}(p, q, r)$ in [3] and [4]. The continuous variables ϕ_j correspond to the discrete state variables a, b, c, d and the integral $\sqrt{\beta/\pi} \int d\phi_0$ to the sum \sum_d there.

In the zero-temperature limit $\beta \rightarrow \infty$ the integral in the LHS of [37] is dominated by the maximum of the integrand and the RHS is also dominated by the exponential. The star-triangle relation [1], [2] emerges, when identifying $R_{j,0} = Z_j$, ($j = 1, 2, 3$), and $R_{1,2} = \bar{Z}_3$, $R_{2,3} = \bar{Z}_1$, $R_{3,1} = \bar{Z}_2$ in [38].

Another mapping has been given by Fortuin and Kasteleyn, who have shown that any planar resistor network is related to an $N \rightarrow 0$ limit of a corresponding N -state Potts model [See, e.g., Section IV C of F.Y. Wu, Rev. Mod. Phys. 54, 235–268 (1982)]. Given Potts interaction energy

$$\mathcal{E} = - \sum_{\langle j, j' \rangle} J_{j, j'} \delta_{\sigma_j, \sigma_{j'}}, \quad [39]$$

we make, for each edge $r = \langle j, j' \rangle$, the special combinations

$$x_r = \frac{e^{\beta J_r} - 1}{\sqrt{N}}, \quad \bar{x}_r = \frac{e^{\beta \bar{J}_r} - 1}{\sqrt{N}} \equiv \frac{1}{x_r}. \quad [40]$$

The last equation defines the corresponding coupling constant \bar{J}_r of the dual Potts model. The limit $N \rightarrow 0$ is defined via the six-vertex model and in this limit we may choose $\beta = \sqrt{N}$ and find

$$x_r = J_r = c/R_r, \quad \bar{x}_r = \bar{J}_r = c/\bar{R}_r, \quad [41]$$

with c some positive constant.

Writing the star-triangle equation [3] for the N -state Potts model in terms of x and \bar{x} with

$$W_{ab}(p, q) = 1 + \sqrt{N}x(p-q)\delta_{a,b}, \quad \bar{W}_{ab}(p, q) = 1 + \sqrt{N}\bar{x}(p-q)\delta_{a,b}, \quad [42]$$

we find five independent equations. Eliminating $R(p, q, r)$, we arrive at

$$\begin{aligned} \bar{x}(p-q)x(p-r)\bar{x}(q-r) &= \bar{x}(p-q) + x(p-r) + \bar{x}(q-r) + \sqrt{N}, \\ \text{and } x(u)\bar{x}(u) &\equiv 1, \end{aligned} \quad [43]$$

with the well-known solution $x(u) = \sin(u)/\sin(\theta-u) = 1/\bar{x}(u)$, where $\theta \equiv \arccos(\sqrt{N}/2)$. In the limit $N \rightarrow 0$ this solution becomes $x(u) = \tan(u)$, $\bar{x}(u) = \cot(u)$, while, in view of [41], Eq. [43] reduces to [1] and [2] with

$$\begin{aligned} Z_1 &= c \tan(p-q), & Z_2 &= c \cot(p-r), & Z_3 &= c \tan(q-r), \\ \bar{Z}_1 &= c \cot(p-q), & \bar{Z}_2 &= c \tan(p-r), & \bar{Z}_3 &= c \cot(q-r). \end{aligned} \quad [44]$$

This is a rapidity parametrization of the solution of [1] and [2].